



PERGAMON

Available online at www.sciencedirect.com

SCIENCE @ DIRECT®

Solid State Communications 127 (2003) 535–539

solid
state
communicationswww.elsevier.com/locate/ssc

Influence of the electron-lattice coupling for Cr³⁺ ions in Nb⁵⁺ site into congruent co-doped LiNbO₃: Cr³⁺: ZnO crystal

G.A. Torchia^{a,b,c,*}, O. Martinez Matos^{a,b}, P. Vaveliuk^d, J.O. Tocho^{b,c}^aDepartamento de Física de Materiales Universidad Autónoma de Madrid, Spain^bCentro de Investigaciones Ópticas CC124, La Plata, 1900 Argentina^cDepartamento de Física, Facultad de Ciencias Exactas, Universidad Nacional de La Plata, Buenos Aires, Argentina^dDepartamento de Física, Centro de Ciências Exatas e da Natureza, Universidade Federal da Paraíba, Caixa Postal 5008, CEP 58051-970 3020 Pessoa, PB, Brazil

Received 4 February 2003; received in revised form 20 May 2003; accepted 17 June 2003 by J.F. Sadoc

Abstract

This paper shows the important role that plays the electron-lattice coupling to represent correctly the energy levels of Cr³⁺ ions in Nb⁵⁺ site into congruent LiNbO₃ crystals doped with 5.3% of ZnO. Racah's parameters: $B = 646 \text{ cm}^{-1}$, $C = 3022 \text{ cm}^{-1}$ and crystal field intensity $Dq = 1342 \text{ cm}^{-1}$ were determined and the Tanabe–Sugano's diagram was constructed. The characteristics of the absorption and emission spectra of Cr³⁺ ions in Nb⁵⁺ site have been explained in terms of the Configurational Co-ordinate model in the harmonic approximation. Huang–Rhys parameter, $S = 3.5$ and the breathing phonon energy, $\hbar\omega = 460 \text{ cm}^{-1}$, are also reported in this work. Different values of breathing phonon for Cr³⁺ in Nb⁵⁺ site than in Li⁺ site could explain the higher luminescent quantum efficiency of Cr³⁺ ions located in Nb⁵⁺ site in LiNbO₃ crystals.

© 2003 Elsevier Ltd. All rights reserved.

PACS: 61.72 – y; 42.62.Fi; 63.20.Kr

Keywords: A. Cr³⁺ impurities; A. LiNbO₃ crystals; D. Phonon electron interaction; E. Laser spectroscopy

1. Introduction

The lithium niobate (LNB) crystals doped with transition metals and/or rare earth ions have been studied in the last 10 years to achieve new laser and non-linear optical devices. The photorefractive damage effect that present in LNB is a severe problem for laser applications that could be suppressed by adding at about 5% of MgO or ZnO in the crystal [1]. Several examples of high efficiency lasers based on double doped lithium niobate have been recently reported [2,3].

Cr³⁺ ions is a good candidate to dope LNB in order to obtain broad spectral tunable lasers which arise from its wide emission band due to the strong lattice coupling [4].

Early work, by using Electron Paramagnetic Resonance

(EPR) in congruent Cr³⁺: LiNbO₃ crystal has determined that the Cr³⁺ ions prefer to occupy the Li⁺ site in the LiNbO₃ lattice [5]. More recently papers by means of optical experiments such as excitation, emission and time resolved spectroscopy, have confirmed this result [6,9]. For near stoichiometric Cr³⁺: LiNbO₃ crystals, the majority Cr³⁺ centre is also reported to be Cr³⁺ in Li⁺ site performed by means of the analysis of the R-lines emission [8–10].

Likewise, the congruent lithium niobate crystals are doped with Mg²⁺ or Zn²⁺ impurities in order to suppress the photorefractive effect. For a cation concentration up to the threshold (~4.6%) the Cr³⁺ ions prefer to occupy principally the Nb⁵⁺ site in the lattice as it was observed by and Electron Nuclear Double Resonance and EPR experiments [5,11,12]. This new Cr³⁺ centre has been also confirmed by using optical [12–14] and Rutherford Backscattering techniques [15]. For stoichiometric Mg²⁺ co-doped LiNbO₃: Cr³⁺ crystals the Cr³⁺ redistribution from Li⁺ to Nb⁵⁺ site was estimated for a cation concentration of 0.2 mol% [16].

* Corresponding author. Current address: Departamento de Física de Materiales C-IV, Universidad Autónoma de Madrid, 28049 Cantoblanco, Madrid, Spain. Tel.: +34-91-397-3818; fax: +34-91-397-8579.

E-mail address: gustavo.torchia@uam.es (G.A. Torchia).

For the crystal used in this work, the both Cr^{3+} centres coexist having approximately 80 and 20% for Cr^{3+} in Nb^{5+} and Cr^{3+} in Li^+ site, respectively. These results were obtained by using EPR techniques [14].

At both sites the Cr^{3+} experiments a nearly octahedral electric field produced by two planes of O^{2-} ligands. As it is known the influence of crystal field is very strong on transition metals ions because the extended $3d^n$ electron configuration is substantially affect by this field. The energy levels for different d^n electron configuration in a rigid environment with one octahedral co-ordination lattice have been calculated by Tanabe and Sugano [17]. Energy values are tabulated in terms of the Racah's parameters A , B and C and the crystal field Dq [18].

The lowest excited energy state for many chromium systems is 2E state. This kind of transitions occurs without phonons coupling, showing a characteristic narrow luminescence band (R lines) [19]. However, the Cr^{3+} ions in LNB crystals show a characteristic broad band emission corresponding to ${}^4T_2 \rightarrow {}^4A_2$ vibronic transitions [13].

Purely electronic transitions in perfect crystals have linewidths determined entirely by lifetime and dephasing mechanisms. The interaction between optically active impurity ions and the vibration of the host lattice is of great importance to understand optical transitions in real crystals.

In this paper, we present the absorption and emission characteristics of Cr^{3+} ions in Nb^{5+} site into congruent lithium niobate co-doped with ZnO taking into account the electron-lattice coupling in terms of the configurational coordinate breathing model in the harmonic approximation. The Huang–Rhys parameter (S) and the breathing phonon energy ($\hbar\omega$) are determined in base of this model.

2. Experimental procedure

The sample used in this work was grown by Czochralski method in open air atmosphere standing with Li_2O and Nb_2O_5 amounts that assure congruent concentrations in the crystal. The concentration doping in the melt were 8% for ZnO and 0.15% for Cr_2O_3 . The composition in the crystals was analysed by EXTF (Fluorescence Total X-ray Emission) giving 0.1 and 5.3% for Chromium and Zinc ions, respectively, normalised to Nb^{5+} concentrations. Samples was cut in slices of 1 mm width, reduced to dices of $1 \times 4 \times 6 \text{ mm}^3$ and polished with diamond powders of different diameters.

The continuous wave emission spectrum was performed at room temperature buy using an Argon laser at 514 nm in order to principally excite the Cr^{3+} (Nb^{5+}) centre. The signals were detected with an AsGaIn (Hamamatsu 751 K) cooled photomultiplier. The luminescence was dispersed by 0.5 m monochromator (SPEX 500M) and amplified by a lock-in (EE&G). The absorption and emission spectra were

analysed with a multi-gaussian fitting and energy levels reported below correspond to peak values of fitting.

3. Results and discussion

Fig. 1 shows the absorption and emission spectra at room temperature for the centres of Cr^{3+} ions in Nb^{5+} site into congruent lithium niobate crystals co-doped with Cr^{3+} and ZnO (5.3%). The absorption spectrum was taken from Ref. [14] which it was resolved for this optical centre. It shows two broad bands centred at $19,550 \text{ cm}^{-1}$ (511 nm) and $13,421 \text{ cm}^{-1}$ (745 nm) associated with vibronic transitions of the Cr^{3+} ions in Nb^{5+} site in LNB crystal. The band centred at 511 nm is associated with ${}^4A_2 \rightarrow {}^4T_1$ transition while the band centred at 745 nm is associated to ${}^4A_2 \rightarrow {}^4T_2$ transition, both bands are spin allowed transitions.

As seen in Fig. 1, the emission spectrum presents a broad band centred at $10,484 \text{ cm}^{-1}$ (954 nm); this band was associated with the transition ${}^4T_2 \rightarrow {}^4A_2$ that principally corresponds to Cr^{3+} ions in Nb^{5+} site centre [13].

From the absorption spectrum shown in Fig. 1, the strength of the octahedral crystal field Dq , and the spectroscopic Racah's parameters B and C are calculated. It is well known that Dq is obtained directly from the energy corresponding to the peak of the ${}^4A_2 \rightarrow {}^4T_2$ absorption band, which is equal to $10 Dq$,

$$Dq = [E({}^4T_2) - E({}^4A_2)]/10 = 1342 \text{ cm}^{-1}. \quad (1)$$

Considering ΔE as the energy difference between the 4T_2 and the lowest 4T_1 state, that experimentally is the separation between the two strong absorption bands in

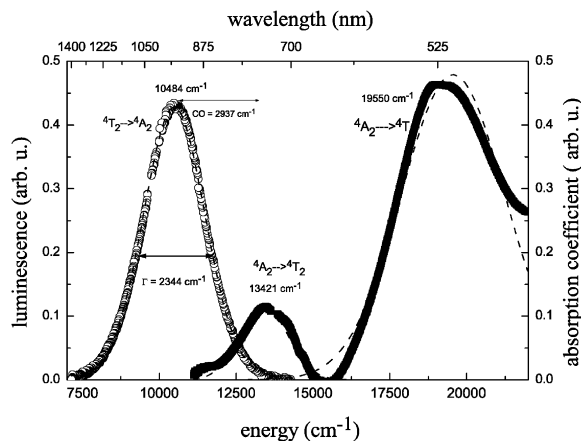


Fig. 1. Room temperature absorption and luminescence spectra of Cr^{3+} ions in Nb^{5+} sites. Energy values of relevant levels, the Stokes shift (CO) and the FWHM bandwidth (I) of the emission band are indicated.

Fig. 1, the B value is obtained from,

$$\frac{B}{Dq} = \frac{\left(\frac{\Delta E}{Dq}\right)^2 - 10\left(\frac{\Delta E}{Dq}\right)}{15\left(\frac{\Delta E}{Dq} - 8\right)}, \quad (2)$$

for $Dq = 1342 \text{ cm}^{-1}$ and $\Delta E = 6129 \text{ cm}^{-1}$, the result $B = 646 \text{ cm}^{-1}$ is obtained.

The last Racah's parameter can be calculated from an approximate expression given by Henderson e Imbusch [19]

$$C = [E(^2E) - 7.9B + 1.8B^2/Dq]/3.05; \quad (3)$$

Using the experimental value for the energy corresponding to the 2E level, $E(^2E) = 13,755 \text{ cm}^{-1}$ from Ref. [14] and the values found previously for Dq and B , the result $C = 2951 \text{ cm}^{-1}$ is obtained. Exact determination of C requires the diagonalization of the 4×4 matrix corresponding to the 2E states given in Ref. [18]. The lowest eigenvalue gives the analytical expression necessary to calculate $C = 3022 \text{ cm}^{-1}$ by solving a transcendental equation.

Table 1 shows the Racah parameters and the crystal field intensity for each Cr^{3+} centres in LNB crystals. As it can be seen the main difference lies over the Dq/B ratio which reveals the crystals field zone for each Cr^{3+} centre.

With the Racah's parameters found above, the energy for the most relevant states, taking the energy of the 4A_2 state equal to zero, can be calculated from Eqs. (1)–(3),

$$\left. \begin{aligned} E(^4A_2)/B &= 0, \\ E(^4T_2)/B &= 10/a, \\ E(^4T_1)/B &= \{20 + 15a - [(10 + 15a)^2 - 480a]^{1/2}\}/2a, \\ E(^2E)/B &= 3.05 C/B + 7.90 - 1.80a, \end{aligned} \right\} \quad (4)$$

where $a = B/Dq$.

The Tanabe–Sugano diagram constructed in this manner for the main spectroscopic states of Cr^{3+} in Nb^{5+} site is presented in Fig. 2. The vertical broken line represents the appropriate value for Dq/B (2.1) found for this centre. In this figure we have also included exact solution for the 2E energy state (dashed line) calculated from the energy matrices [18].

We have made this new diagram instead of the one reported previously for centre of Cr^{3+} in Li^+ site [20] because the new Cr^{3+} position in LiNbO_3 lattice is situated

Table 1

Racah parameters B and C and the crystals field intensity Dq for $\text{Cr}^{3+}(\text{Li}^+)$ and $\text{Cr}^{3+}(\text{Nb}^{5+})$ centres in $\text{LiNbO}_3:\text{ZnO}(5.3\%)$ crystals

	$\text{Cr}^{3+}(\text{Li}^+)$	$\text{Cr}^{3+}(\text{Nb}^{5+})$
$Dq \text{ (cm}^{-1}\text{)}$	1527	1342
$B \text{ (cm}^{-1}\text{)}$	533	646
$C \text{ (cm}^{-1}\text{)}$	3244	3022
Dq/B	2.9	2.1

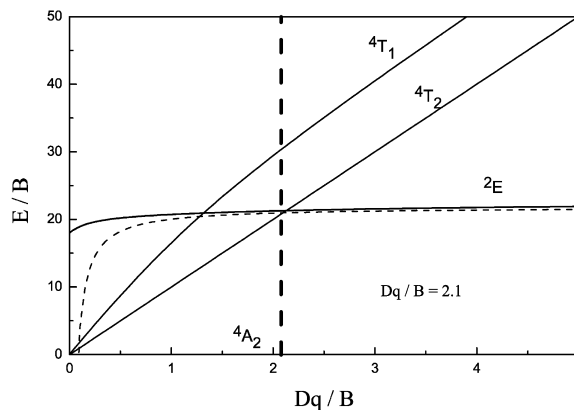


Fig. 2. Tanabe–Sugano's diagram for Cr^{3+} in Nb^{5+} sites. The solid line for 2E level corresponds to the exact diagonalization of the matrix from Ref. [13], while the dashed line is the approximation given by Eq. (3).

closer to the oxygen octahedral centre and it could make substantially differences for emission and absorption spectrum.

Over this diagram, it is not clear which is the lowest energy level at $Dq/B = 2.1$ since the broken line pass through the cross-over point between the 4T_2 and 2E states. We interpret this fact as both states could be emitter levels in contradiction with experimental results found in this paper since from the emission spectrum we observe only luminescence broad band corresponding to the $^4T_2 \rightarrow ^4A_2$. To justify this controversy satisfactory we must consider a more complex model taking into account the electron-lattice coupling. As the first approximation, the vibrating environment can be modelled by the Configurational Co-ordinate model in the harmonic approximation.

The Configurational Co-ordinate model assumes that the distance Q from the active ion to its first shell of neighbouring oxygen ions pulsates harmonically about its equilibrium value Q_0 . As a further approximation the same breathing frequency is considered for all the electronic potential. Equilibrium values for Q are specific for each electronic potential. The Q difference between the ground parabola and the excited parabola minimum is proportional to the number of the coupling phonons in the electronic transitions. As wider the spectrum is, larger will be the coupling between electronic states. As usual, the difference in electron-lattice coupling is characterised by a dimensionless constant, the Huang–Rhys parameter S , defined as the number of vibrating quanta excited in the most probable absorption transition ($S = E_{\text{dis}}/\hbar\omega$, where E_{dis} is defined in Fig. 3).

For the determination of the phonon energy and the Huang–Rhys parameter we used the spectroscopic data of Fig. 1. The absorption and emission bands from transitions that connect the 4A_2 and 4T_2 states are approximately Gaussians, for this case the Stokes shift, the difference in energy between the absorption and emission band peaks,

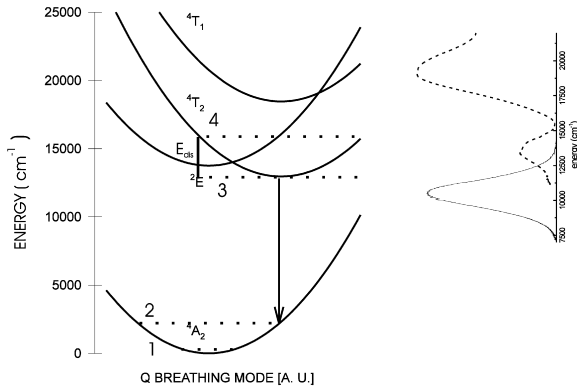


Fig. 3. Coordinate configurational diagram of Cr^{3+} ions in Nb^{5+} sites in LN crystals. The dashed lines represents the four level system considered for this centre.

can be related with S by mean of the following expression,

$$\text{CO} = (2S - 1)\hbar\omega, \quad (5)$$

where CO means the Stokes shift. Other equation necessary to calculate the phonon energy and the Huang–Rhys parameter is given by the expression of the bandwidth

$$\Gamma(T) = 2.35\hbar\omega(S \coth(\hbar\omega/kT))^{1/2}, \quad (6)$$

where $\Gamma(T)$ stands for the FWHM of the emission band; $k = 0.695 \text{ cm}^{-1} \text{ K}^{-1}$ is the Boltzman's constant. Using Eqs. (5) and (6) and the values found experimentally for the Stokes shift and the bandwidth ($\text{CO} = 2937 \text{ cm}^{-1}$, $\Gamma(T) = 2344 \text{ cm}^{-1}$), we get $\hbar\omega = 460 \text{ cm}^{-1}$ and $S = 3.5$ for $T = 295 \text{ K}$.

Configurational Co-ordinate scheme of Cr^{3+} in Nb^{3+} site is sketched in Fig. 3. It is obtained in a pictorial way, which represents correctly the absorption and emission spectrum for this emitter centre in LNB crystals. This diagram reveals that taking into account the electron-lattice coupling the lowest of the electronic energy potential corresponds to the ${}^4\text{T}_2$ state in accordance with the experimental results shown in this work. Likewise this representation shows that the Cr^{3+} (Nb^{5+}) centre can be considered as a four level system since the vibronic excited corresponding to ${}^4\text{A}_2$ manifold has been estimated to be around at 2100 cm^{-1} higher than kT energy at room temperature (200 cm^{-1}).

4. Conclusions

In this paper, we have presented the crystal field strength, the spectroscopic Racah's parameters, the Huang–Rhys parameter and the breathing phonon frequency corresponding to the centers of Cr^{3+} ions in Nb^{5+} site in congruent LNB crystal. Dq and Racah parameters (B and C) are found similarly to previously reported for other lithium niobate samples [7,21] and in particular to one corresponding to the centres of Cr^{3+} in Li^+ site [20].

We show the importance to consider the coupling electron-lattice to interpret the correct position of the energy level of Cr^{3+} ions in this crystal. Breathing phonon energy for Cr^{3+} in Nb^{5+} site was determined to our knowledge for the first time.

In this paper, we can also explain the luminescence quantum efficiency (Φ) difference between Cr^{3+} in Li^+ ($\Phi \approx 5\%$) and Nb^{3+} ($\Phi \approx 10\%$) sites [22]. For both centres many phonons are involved in the optical transition ${}^4\text{T}_2 \rightarrow {}^4\text{A}_2$ thus higher quantum efficiency luminescence should be find for both emitter centres. This prediction is a contradiction since both centres have low luminescence quantum efficiencies [22]. This controversy could be explained taking into account the coupling of breathing phonons with bulk normal vibrations, as it was suggested in a previous work [20]. In particular, the Cr^{3+} in Li^+ site have stronger coupling than for Cr^{3+} in Nb^{5+} site in LNB crystals [23], for this reason the last centre is a bit more luminescence. In a brief, the breathing phonon for Cr^{3+} in Nb^{5+} centres (460 cm^{-1}) have a weak coupling with the normal bulk vibrations in LNB located at 432 cm^{-1} (TO), at 424 cm^{-1} and 456 cm^{-1} (LO) as it is shown in the paper developed by Ridah et al. [23].

Acknowledgements

G.A. Torchia wishes to acknowledge the CONICET (Argentina) for his fellowship.

References

- [1] T.R. Volk, N.M. Rubinina, V.I.M. Wöhlecke, J. Opt. Soc. Am. B 11 (1994) 1681–1687.
- [2] D. Jaque, J. Capmany, J. García-Solé, A. Brenier, G. Boulon, Appl. Phys. B 70 (2000) 11–14.
- [3] E. Montoya, J. Capmany, L.E. Bausá, T. Kellner, A. Diening, G. Haber, Appl. Phys. Lett. 74 (21) (1999) 3113–3115.
- [4] Y. Qui, J. Phys.: Condens. Matter 5 (1993) 2041.
- [5] A. Martín, F.J. López, F. Agulló-López, J. Phys.: Condens. Matter 4 (1992) 847–853.
- [6] A. Kaminska, J.E. Dmochowski, A. Suchoki, J. Garcia-Sole, F. Jaque, L. Arizmendi, Phys. Rev. B 60 (1999) 7707–7710.
- [7] P. Macfarlane, K. Holladay, J.F.H. Nicholls, B. Henderson, J. Phys.: Condens. Matter 7 (1995) 9643–9656.
- [8] G.M. Salley, S.A. Basun, G.F. Imbusch, A.A. Kaplyanskii, S. Kapphan, R.S. Meltzer, U. Happek, J. Lumin. 83–84 (1999) 423–427.
- [9] F. Lhomme, P. Bourson, G. Boulon, Y. Guyot, M.D. Fontana, Eur. Phys. J. Appl. Phys. 20 (2002) 29–40.
- [10] T.P.J. Han, F. Jaque, V. Bermudez, E. Dieguez, J. Phys.: Condens. Matter 15 (2003) 281–290.
- [11] G. Corradi, H. Soethe, J.M. Spaeth, K. Polgár, J. Phys.: Condens. Matter 3 (1991) 1901–1908.
- [12] J. Diaz-Caro, J. García-Solé, D. Bravo, J.A. Sanz-García, F.J. López, F. Jaque, Phys. Rev. B 54 (18) (1996) 13042–13046.

- [13] G.A. Torchia, J.A. Sanz-García, J. Díaz-Caro, T. Han, F. Jaque, *Chem. Phys. Lett.* 288 (1998) 65–70.
- [14] G.A. Torchia, J.O. Tocho, F. Jaque, *J. Phys.: Condens. Matter* 12 (41) (2000) 8927–8932.
- [15] A. Kling, J.C. Soares, M.F. da Silva, J.A. Sanz-García, E. Dieguez, F. Agulló-López, *Nucl. Instrum. Meth. Phys. Res., Sec. B—Beam Interact. Mater. Atoms* 136–138 (1998) 426–430.
- [16] G.A. Torchia, J.A. Sanz-García, F.J. López, D. Bravo, J. García-Solé, F. Jaque, H.G. Gallagher, T.P.J. Han, *J. Phys.: Condens. Matter* 10 (1998) L341–L345.
- [17] Y. Tanabe, S. Sugano, *J. Phys. Soc. Jpn* 9 (1954) 753.
- [18] S.J. Sugano, Y. Tanabe, H. Kamikura, *Multiplets of Transitions Metals Ions in Crystals*, Academic Press, New York, 1970.
- [19] B. Henderson, G.F. Imbush, *Optical Spectroscopy of Inorganic Solids*, Oxford Science Publications, 1989.
- [20] G.A. Torchia, O. Martínez Matos, P. Vaveliuk, J.O. Tocho, *J. Phys.: Condens. Matter* 13 (30) (2001) 6577–6583.
- [21] E. Camarillo, J.O. Tocho, I. Vergara, E. Dieguéz, J. García-Solé, F. Jaque, *Phys. Rev. B* 45 (1990) 4600–4604.
- [22] G.A. Torchia, J.A. Muñoz, F. Cusso, F. Jaque, J.O. Tocho, *J. Lumin.* 92 (2001) 317–322.
- [23] A. Ridah, P. Bourson, M.D. Fontana, G. Malovichko, *J. Phys.: Condens. Matter* 9 (1997) 9687–9693.